Functional expression of a low-affinity zinc uptake transporter (*Fr*ZIP2) from pufferfish (*Takifugu rubripes*) in MDCK cells

Andong QIU and Christer HOGSTRAND[1]

King's College London, Nutritional Sciences Research Division, Franklin-Wilkins Building, 150 Stamford Street, London SE1 9NH, U.K.

Zinc is a vital micronutrient to all organisms and it is therefore very important to determine the mechanisms that regulate cellular zinc uptake. Previously, we reported on zinc uptake transporters from zebrafish (*Danio rerio*; *Dr*ZIP1) and *Fugu* pufferfish (*Takifugu rubripes*; *Fr*ZIP1) that facilitated cellular zinc uptake of high affinity ($K_m < 0.5$ μM) in both CHSE214 [chinook salmon (*Oncorhynchus tshawytscha*) embryonic 214] cells and *Xenopus laevis* oocytes. To investigate additional biochemical pathways of zinc uptake in fish, we molecularly cloned the second fish member (*Fr*ZIP2) of the SLC39 subfamily II from *Fugu* pufferfish gill. Functional characterization suggests that *Fr*ZIP2 stimulated zinc uptake in a temperature-, time-, concentration- and pH-dependent manner when overexpressed in MDCK cells (Madin–Darby canine kidney cells). In comparison with *Fr*ZIP1 and *Dr*ZIP1 (< 0.5 μM), *Fr*ZIP2 appears to represent a low-affinity zinc uptake transporter ($K_m = 13.6$ μM) in pufferfish. *Fr*ZIP2 protein was selective for zinc, but it might also transport Cu^{2+}, since 20 times excess of Cu^{2+} completely abolished its zinc uptake activity. The zinc uptake by *Fr*ZIP2 was stimulated in a slightly acidic medium (pH 5.5–6.5) and was completely blocked at pH 7.5 and above, suggesting that an inward H^+ gradient might provide a driving force for zinc transport by *Fr*ZIP2. Furthermore, *Fr*ZIP2-mediated zinc uptake activity was slightly inhibited by 0.5 mM HCO_3^-, indicating that *Fr*ZIP2 may employ a different mechanism of zinc translocation from the assumed HCO_3^--coupled zinc transport used by human SLC39A2. The *FrZIP2* gene was expressed in all the tissues studied herein, with especially high levels in the ovary and intestines. Thus *Fr*ZIP2 may be a prominent zinc uptake transporter of low affinity in many cell types of *Fugu* pufferfish.

Key words: copper, influx, MDCK cell, pufferfish, SLC39A3, zinc uptake transporter.

INTRODUCTION

Zinc is an essential micronutrient to all organisms by participating in protein, nucleic acid, carbohydrate and lipid metabolism, as well as in the control of gene transcription and co-ordination of other biological processes [1]. Due to its functional importance, zinc balance has to be precisely regulated to satisfy the proper demands of the normal physiological functions for zinc, and the loss of zinc balance can result in serious damaging consequences. It has been found that even moderate zinc deficiency can cause problems, including anaemia, loss of appetite, immune system defects, developmental problems and teratogenesis [2]. Conversely, excessive zinc accumulation can be toxic and has been linked to neurodegeneration [3]. Furthermore, zinc pollution is an environmental problem with the high frequency of water quality criteria violation in Europe and the U.S.A.

Consistent with the essential yet toxic nature of zinc, cells harbour mechanisms for homoeostatic zinc control with respect to uptake, excretion and distribution. Zinc uptake across the apical membrane of absorptive epithelial cells is the first gate to regulate zinc homoeostasis in vertebrates [4,5]. Uptake of zinc in fish much resembles that in mammals [5]. There is, however, at least one notable difference between the two groups in this regard. Whereas the intestine is an important zinc uptake site in both fish and mammals, fish also take up zinc across their gills. Like in mammals, the dietary zinc absorption in fish intestine is a carrier-mediated process that follows Michaelis–Menten kinetics [5]. The branchial zinc uptake is also a carrier-mediated transcellular process, thought to primarily take place in discrete 'mitochondria-rich' ionocytes, called chloride cells [4,5]. Correspondingly, a group of transporter proteins exist to mediate cellular zinc uptake in the evolutionarily diverse organisms (yeast, plants and mammals) [6,7]. These proteins are from the large ZIP family of transporters [derived from ZRT1-, IRT1 (iron-regulated transporter 1)-like protein] [8], and play roles in transport of zinc from outside the cell into the cytoplasm [6,7]. ZIP transporters have also been found to mobilize stored zinc by transporting the metal from endosomes or vacuoles into the cytosol [9,10]. The ZIP family has recently been given a systematic name, SLC39A (solute carrier family 39A), which is composed of four separate subfamilies of transporter proteins [11]. Subfamily I contains mainly fungal and plant sequences, while subfamily II consists of mammalian, nematode and insect genes [6,7]. Subfamily III (gufA subfamily), is a group of prokaryote and eukaryote proteins related to the gufA gene of *Myxococcus xanthus*, which has unknown function. Most ZIP subfamily III proteins have not been functionally characterized except the yeast ZRT3, which translocates zinc from the vacuole to the cytoplasm in yeast [9]. The fourth subfamily, also named LIV-1 subfamily of ZIP zinc transporters (LZT), is related to the oestrogen-regulated gene LIV-1 that facilitates cellular zinc uptake in glandular tissues [7]. Thus ZIP proteins appear to represent an impressive array of

Abbreviations used: CHSE214, chinook salmon (*Oncorhynchus tshawytscha*) embryonic 214; ECaC, epithelial calcium channel; MDCK cells, Madin–Darby canine kidney cells; ORF, open reading frame; RACE, rapid amplification of cDNA ends; RT, reverse transcriptase; SLC39A, solute carrier family 39A; TM, transmembrane.

[1] To whom correspondence should be addressed, at School of Health and Life Sciences, King's College London, Franklin-Wilkins Building, 150 Stamford Street, London SE1 9NN, U.K. (email christer.hogstrand@kcl.ac.uk).

The nucleotide sequence data reported will appear in DDBJ, EMBL, GenBank® and GSDB Nucleotide Sequence Databases under the accession number AY529486.

molecular mechanisms in zinc homoeostasis at diverse phylogenetic levels.

In mammals, SLC39A4 (ZIP4), a member of the LZT subfamily, is a likely mediator of dietary zinc uptake in the intestines and is dynamically regulated by dietary zinc at both transcriptional and post-translational levels [12–14]. It remains to be established whether or not there are orthologues of SLC39A4 in fish. Mutations of SLC39A4 in humans are related to the disease AE (acrodermatitis enteropathica), which is characterized by decreased zinc uptake in the small intestine and other cells of the body and an autosomal recessive pattern of inheritance [13,14]. However, the dysfunctional SLC39A4 only reduces zinc uptake and does not completely abrogate the dietary zinc absorption [13,14], suggesting that there are probably alternative pathways for zinc uptake in the intestines. Three members of the ZIP subfamily II (SLC39A1, SLC39A2 and SLC39A3) have so far been functionally characterized in mammals [11,15–17]. The relative abundance of the respective mRNA for these proteins in intestine of mouse does not seem to be dramatically changed in response to zinc deficiency [17,18]. However, zinc supplementation in human subjects was found to reduce SLC39A4 protein in the intestine [19]. Recent evidence suggests that post-translational events may play an important role in controlling cellular zinc influx. Zinc uptake mediated by SLC39A1, SLC39A3 and SLC39A4 appears to be regulated through trafficking of these transporters between the plasma membrane and intracellular compartments [20,21]. Lowering the zinc availability to cultured mouse cells resulted in a decreased rate of endocytosis of these proteins and a resulting increased localization to the plasma membrane. Two closely related members of the ZIP subfamily II, *Dr*ZIP1 and *Fr*ZIP1, have recently been molecularly cloned from the gills of zebrafish and pufferfish respectively [22]. Both of these are similar to human and mouse SLC39A1 and SLC39A2. *Dr*ZIP1 acted as a high-affinity zinc uptake transporter when expressed in either CHSE214 cells [chinook salmon (*Oncorhynchus tshawytscha*) embryonic 214 cells] or *Xenopus laevis* oocytes [22]. As both *DrZIP1* and *FrZIP1* genes are expressed in the gill and the intestine, their proteins may mediate a pathway of cellular zinc absorption in these tissues [22]. ECaC (epithelial calcium channel; TRPV6) seems to be another pathway of zinc uptake from the water in fish gills [23]. ECaC mediates a shared route for zinc and calcium uptake [23] that was previously inferred in the gill, but not the intestine, by using physiological methodologies [4]. This is consistent with the finding that expression of ECaC in fish is high in gills and low in intestine [23]. In the present study, we identified and functionally characterized a second member of the ZIP subfamily II (*Fr*ZIP2) from the gill of pufferfish, *Takifugu rubripes*. The results suggest that *Fr*ZIP2 protein is similar to human and mouse SLC39A3 and that it mediated low-affinity zinc uptake when expressed in MDCK (Madin–Darby canine kidney) cells. Although a large number of slc39A genes have now been identified, there is little information on the biochemical mechanisms by which their respective proteins operate. We present novel functional information showing that the transport activity of the *Fugu* SLC39A3 orthologue, *Fr*ZIP2, is inhibited by HCO_3^- and by pH above neutral. Consistent with published information on mouse ZIP3 [20], zinc transport by *Fr*ZIP2 was markedly inhibited by copper.

EXPERIMENTAL

Cloning of the ZIP homologue from *Fugu* pufferfish gill

Total RNA from gill, intestine, kidney and ovary of *Fugu* pufferfish was obtained from HGMP-RC (Human Genome Mapping Project Resource Centre) of the Medical Research Council (MRC), Cambridge, U.K. The first-strand cDNA was synthesized with Powerscript™ RT (reverse transcriptase) (ClonTech Laboratories, Basingstoke, U.K.) and the primer ADP1 (Table 1).

Table 1 Primers used in reverse transcription and PCRs

V = A, G or C.

Primer	Nucleotide sequence (5′→3′)
*Fr*ZIP2-F	GCAGCTTCAGGATGGACATC
*Fr*ZIP2-R	TCACCACTTGATGAACACGAG
5GSP	TGAGCAGCGGCAGAGACCTC
5NGSP	AGCCGAGTCGGAGCTGAGCAG
3GSP	GCAGCTTCAGGATGGACATC
5NGSP	GTCGGTGGTGCTGCAGGGAC
*Fr*ZIP2$(H)_6$-R	TACAGGATCCTCAATGGTGATGGTGATGATGCCACTTGATGAACACGAGC
*Fr*ORF-F	TGACCTCGAGCACCATGGACATCCTGGTGGCCAAG
*Fr*ORF-R	TACAGGATCCTCACCACTTGATGAACACGAG
ADP1	CTGATCTAGAATTCGCGAAGC$(T)_{17}$V
ADP2	AGCAGTGGTATCAACGCAGAGT$(T)_{17}$V
UAP1	TGATCTAGAATTCGCGAAGC
UAP2	AAGCAGTGGTATCAACGCAGAGT

Mining of MRC-HGMP *Fugu* genome database [24] was performed with the predicted *Fugu* pufferfish ZIP1 protein (*Fr*ZIP1, Genbank® accession no. AAS21267) as the query. Consequently, two genomic sequences, M001226 and S001063, were identified to contain segments with marked homology to *Fr*ZIP1 amino acid sequence. Primers *Fr*ZIP2-F and *Fr*ZIP2-R (Table 1) were then synthesized according to the sequences flanking the predicted *Fr*ZIP2 ORF (open reading frame), and PCR was subsequently performed.

The 3′- and 5′-ends of *Fr*ZIP2 cDNA were amplified by RACE (rapid amplification of cDNA ends)-PCR by the method of Dolphin et al. [25]. The 5′-end of *Fr*ZIP2 cDNA was amplified by PolyA tailing and subsequent 5′-RACE-PCR with gene-specific primers (5GSP and 5NGSP, Table 1) and universal primers (ADP2 and UAP2, Table 1). The 3′-RACE-PCR was performed to amplify the 3′-end of *Fr*ZIP2 cDNA with gene-specific primers (3GSP and 3NGSP) and UAP1 (Table 1). The full-length *Fr*ZIP2 ORF was amplified with Platinum™ *Pfx Taq* polymerase (Invitrogen), and both of its strands were thoroughly sequenced on a capillary DNA sequencer (CEQ2000; Beckman Coulter, High Wycombe, Buckinghamshire, U.K.) to verify its sequence.

Computational analysis

The alignment of the ZIP proteins and the prediction of phylogenetic relationship were generated with the CLUSTAL W method [26]. The hydrophobicity of *Fr*ZIP2 protein was analysed as described by Moller et al. [27]. Potential phosphorylation sites in *Fr*ZIP2 protein were predicted with [28].

Expression constructs

For functional analysis, the full-length *Fr*ZIP2 ORF was amplified with Platinum™ *Pfx Taq* polymerase with primers *Fr*ORF-F and *Fr*ORF-R (Table 1) and subsequently inserted into the XhoI and BamHI sites of the mammalian expression plasmid vector, pIRES2EGFP (ClonTech), to generate pIRES2EGFP-*Fr*ZIP2. The *Fr*ZIP2 ORF was tagged at its C-terminus with a His_6 epitope by PCR with the primers *Fr*ZIP2-F and *Fr*ZIP2(H)6-R (Table 1) and cloned into pIRES2EGFP to generate pIRES2EGFP-*Fr*ZIP2$(H)_6$. The inserted genes in the plasmid constructs above were thoroughly sequenced to verify the reading direction and sequence correctness.

Cell culture

CHSE214 cells (from A.T.C.C., Manassas, VA, U.S.A.) and MDCK cells (gift from Dr A. T. Mckie, King's College London) were grown in Eagle's minimum essential medium (Eagle's salts, L-glutamine and sodium bicarbonate) supplemented with 10 % (v/v) fetal bovine serum (Sigma–Aldrich), 1 % non-essential amino acids and 2 % (v/v) penicillin–streptomycin (Gibco BRL, Paisley, Renfrewshire, Scotland, U.K.). MDCK cells were cultured at 37 °C in 5 % CO_2, while CHSE214 cells were grown at 20 °C in 5 % CO_2.

SDS-urea/PAGE and Western blotting

Expression plasmids, pIRES2EGFP-*Fr*ZIP2(H)$_6$ and pIRES2-EGFP, were transiently transfected into CHSE214 and MDCK cells respectively with Lipofectamine™ reagent (Invitrogen). After 48 h, the transfected cells were lysed in lysis buffer {10 mM Tris/HCl, pH 7.5, 150 mM NaCl, 2 % (w/v) Chaps, 2 mM PMSF, 0.5 mM 4-[2-aminoethyl(1-benzenesulphonyl)-fluoride], 20 μg/ml leupeptin, 10 μg/ml pepstatin and 10 μg/ml aprotinin} and subsequently sonicated. Urea was then added to the cell lysate to a final concentration of 8 M. Protein samples (20 μg of total protein/sample) were resolved by SDS-urea/PAGE (containing 8 M urea). The proteins were blotted on to a nitrocellulose membrane (Schleicher and Schuell, Dassel, Germany) from the gel, and His$_6$-tagged *Fr*ZIP2 proteins were immunodetected by using mouse anti-His antibody solution (1:2000 dilution) and secondary rabbit anti-mouse IgG–horseradish peroxidase conjugate (1:8000 dilution). ECL® Western Blotting System (Amersham Biosciences) was used for the luminol-based detection of horseradish peroxidase-conjugated anti-mouse antibodies on the membrane.

Stable transfection and assays of cellular $^{65}Zn^{2+}$ uptake

Expression plasmids, pIRES2EGFP-*Fr*ZIP2 and pIRES2EGFP, were transfected into MDCK cells with Lipofectamine™ reagent (Invitrogen), and clonally derived stable transfectant MDCK cell lines were generated by combining G418 and green fluorescence selection.

Both MDCK-*Fr*ZIP2 and MDCK-Vec cells were grown in 500 ml flasks to approx. 80 % confluence. These cells were then mildly trypsinized and suspended. The suspended cells were added into 6 ml Falcon tubes ($\sim 4 \times 10^6$/tube), and washed twice with 1 ml of prewarmed uptake buffer (150 mM KCl, 100 mM glucose and 10 mM Hepes, pH 7.0; 37 °C) [16] by centrifugation at 800 ***g*** for 5 min. After incubation in 0.5 ml of prewarmed uptake buffer in a shaking water bath at 37 °C for 5 min, each was added with 0.5 ml of prewarmed uptake buffer containing $^{65}Zn^{2+}$ plus a certain concentration of $ZnCl_2$, and incubated for a further 20 min unless indicated otherwise.

For assessment of the specificity of the *Fr*ZIP2-dependent activity for zinc over other possible metal substrates, the cells were incubated in prewarmed uptake buffer containing 1.5 μM plus 0.028 μCi $^{65}Zn^{2+}$ with or without added competitor metals (10 μM $LaCl_3$, 1 mM $CaCl_2$, 30 μM $CdCl_2$, 30 μM $CoCl_2$, 30 μM $CuCl_2$, 30 μM $FeCl_3$, 30 μM $FeCl_2$ or 30 μM $ZnCl_2$) at 37 °C for 20 min. Stock solutions of the chloride salts of various metals ($LaCl_3$, $CaCl_2$, $CdCl_2$, $CoCl_2$, $CuCl_2$, $FeCl_3$ and $FeCl_2$) were prepared at 10 mM concentration in distilled water, while $ZnCl_2$ stock solution was prepared at 10 mM in 0.02 M HCl. For pH effects on $^{65}Zn^{2+}$ uptake, cells were incubated in prewarmed uptake buffer of different pH values (pH 5.5, pH 6, pH 6.5, pH 7, pH 7.5 or pH 8) containing 1.5 μM plus 0.03 μCi $^{65}Zn^{2+}$ at 37 °C for 20 min. pH levels in uptake buffer were adjusted with 1 M HCl or 1 M NaOH. For assaying the effects of HCO_3^- on $^{65}Zn^{2+}$ uptake, cells were incubated in prewarmed uptake buffer containing 1.5 μM plus 0.03 μCi $^{65}Zn^{2+}$ and either 0 or 0.5 mM $NaHCO_3$ at 37 °C for 20 min. Control cells were incubated in uptake buffer containing 0.5 mM $NaHCO_3$ at 37 °C for 20 min to examine if the addition of HCO_3^- could change the pH level of uptake buffer.

Assays were stopped by washing cells three times in ice-cold washing buffer (150 mM KCl, 100 mM glucose, 1 mM EDTA and 10 mM Hepes, pH 7.0), and cells were lysed in 1 ml of 1 M NaOH. After thoroughly mixing, 20 μl of cell lysate from each assay was diluted 50 times for protein quantification with Bradford reagent (Sigma–Aldrich) and 0.9 ml was taken for radioactivity counting in a LKB1282 CompuGamma counter.

RT–PCR

To examine the tissue distribution of *Fr*ZIP2 mRNA, 2 μg of total RNA from *Fugu* pufferfish gill, gut, kidney and ovary was treated with DNase I (Promega, Chilworth, Southampton, U.K.), repurified with TRI reagent (Sigma–Aldrich), and reverse-transcribed to the first-strand cDNA with Powerscript™ RT (Clontech). *Fr*ZIP2 was amplified by PCR with primers *Fr*ZIP2-F and *Fr*ZIP2-R (Table 1). The cycle conditions were an initial denaturation of 2 min at 94 °C, 30 cycles of 0.5 min at 94 °C, 0.5 min at 58 °C, 2 min at 72 °C, followed by a final extension cycle of 2 min at 72 °C. As a control, a 0.5 kb fragment of β-actin (Ensembl ID: SINFRUG00000081338) was amplified by PCR with the primers ACT-F and ACT-R (Table 1; a gift from Dr M. S. Clark, HGMP-RC, MRC, Cambridge, U.K.), which are specific to sequences in exons 3 and 5 respectively. The β-actin fragment was amplified for 25 cycles of 0.5 min at 94 °C, 0.5 min at 60 °C, 2 min at 72 °C, followed by a final extension cycle of 2 min at 72 °C.

The PCR products were resolved in 1.5 % agarose gels, and the levels of *Fr*ZIP2 mRNA were semi-quantitatively normalized to the corresponding β-actin mRNA levels by using SigmaGel software (Jandel Scientific, Erkrath, Germany).

RESULTS

Structural characterization of *Fr*ZIP2

The cDNA for a ZIP homologue was molecularly cloned from *Fugu* pufferfish gill with a combination of database mining and PCR techniques, and herein named *Fr*ZIP2. *Fr*ZIP2 cDNA is 1573 bp in length including a PolyA tail at its 3′-end, and contains an ORF encoding a protein of 312 amino acids (Figure 1B) with the predicted molecular mass of 33 kDa. The *Fr*ZIP2 cDNA sequence has been submitted to GenBank® database (NCBI) with accession no. AY529486. This sequence appears to correspond to Ensembl gene ID SINFRUG00000155304 in *Fugu* Build 2d.

*Fr*ZIP2 protein shares significant identity with functionally characterized vertebrate members of the ZIP subfamily II, e.g. zebrafish and *Fugu* pufferfish ZIP1 (*Dr*ZIP1 and *Fr*ZIP1; $\sim$30 %), human SLC39A1, SLC39A2 (31 %) and SLC39A3 (60 %). The regions of identity were scattered throughout the length of these predicted proteins (Figure 1B). In contrast, *Fr*ZIP2 protein shares relatively low identity with members of ZIP subfamily I (< 25 %) and very low identity with members of ZIP subfamilies III and IV (< 15 %). Thus *Fr*ZIP2 is a piscine member of the ZIP subfamily II. Accordingly, many conserved structural features in most other members of the ZIP subfamily II can also be found in *Fr*ZIP2 protein, including eight TM (transmembrane) domains and a potential metal-binding motif with a series of

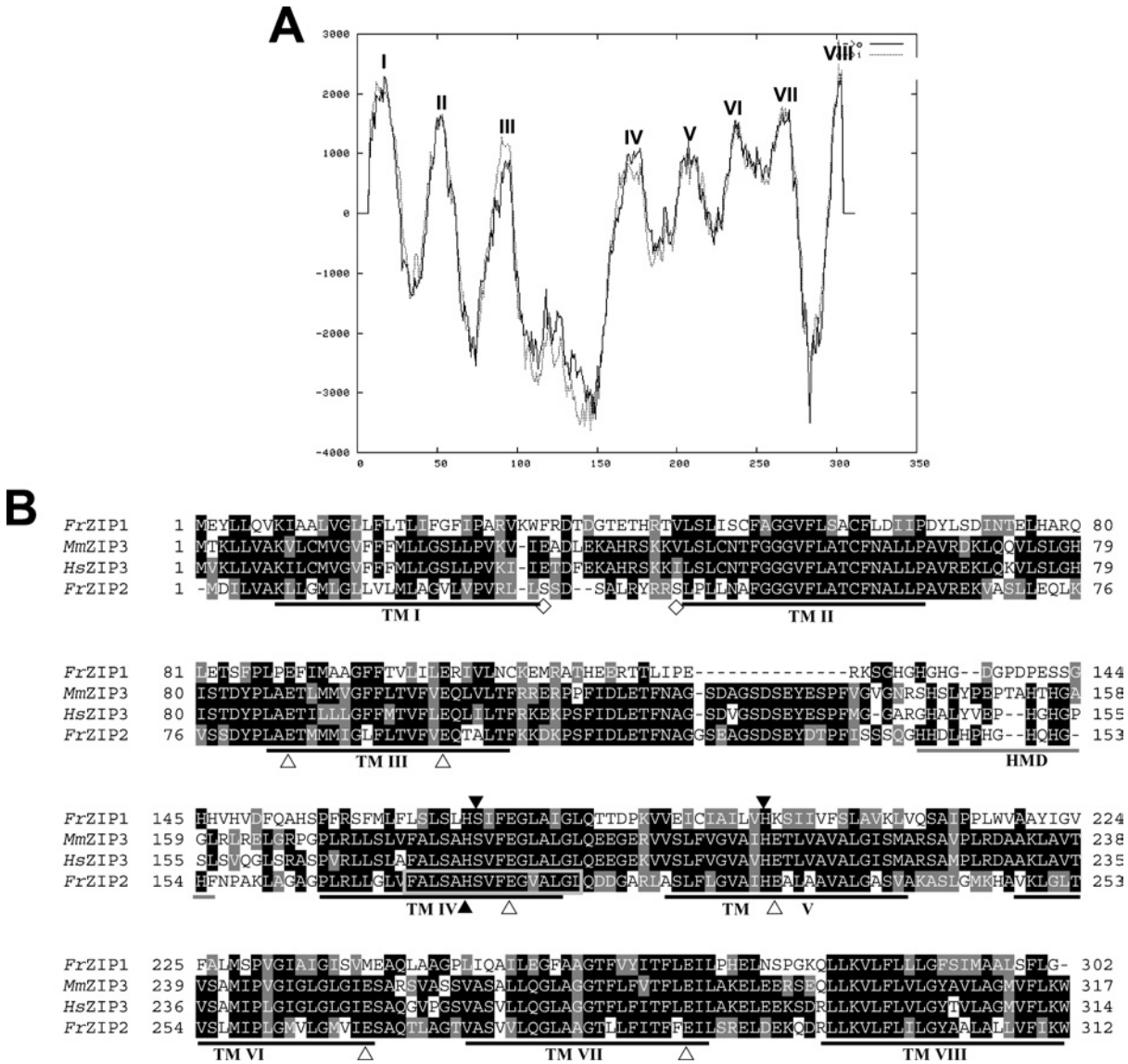

Figure 1 Structural characterization of *Fr*ZIP2 protein

(**A**) Hydrophobicity analysis of pufferfish ZIP transporter 2 (*Fr*ZIP2). Eight TM domains (TM I–VIII) of *Fr*ZIP2 protein are predicted with TMpred (http://www.ch.embnet.org/software/TMPRED_form.html). TM IV and V have low hydrophobicity in comparison with other TMs. The dotted line indicates outside-to-inside topology (N-terminus outside) that is predicted to be the strongly preferred model, and the straight line indicates inside-to-outside orientation (N-terminus inside). (**B**) Alignment of amino acid sequences of *Fr*ZIP2, *Fr*ZIP1 (accession no. AY529485) and mammalian ZIP3 (SLC39A3). *Fr*ZIP2 was aligned with *Fr*ZIP1, human and mouse ZIP3 [accession numbers BC005869 (*Hs*ZIP3) and BC005502 (*Mm*ZIP3)]. Shaded residues represent positions of identity or similarity among the sequences. The eight predicted TM domains are underlined and numbered I–VIII. A potential histidine-rich metal-binding motif between TM III and TM IV is underlined in grey. ▲, conserved functional histidine and serine residues; △, glutamate residues conserved between *Fr*ZIP2 and mammalian ZIP3 proteins; and ◇, potential phosphorylation sites of protein kinase A. Signature sequence of the ZIP family in TM IV of *Fr*ZIP2 is boxed with a grey line. HMD, histidine-rich metal-binding domain.

histidine repeats (HHDLHPHGHQHGH) (Figures 1A and 1B). Furthermore, both TM IV and V of *Fr*ZIP2 protein contain histidine residues that are functionally conserved among most ZIP family members (Figure 1B), and a serine residue in TM IV of *Fr*ZIP2 is conserved in almost all the characterized members of the ZIP subfamilies I and II (Figure 1B). Consistent with the existence of charged and polar residues, TM IV and V of *Fr*ZIP2 are predicted to be amphipathic due to a relatively low hydrophobicity (Figure 1A), which has been thought to be very important for zinc transport mediated by IRT1 [29]. Additionally, there are two glutamate residues in TM II and one in TM IV, V, VI and VII of *Fr*ZIP2 protein (Figure 1B). All of these glutamate residues are surprisingly well conserved in mammalian SLC39A3 proteins (Figure 1B), and may contribute to zinc specificity since glutamate is a good ligand for zinc binding [30]. *Fr*ZIP2 protein also contains two predicted cAMP-dependent protein kinase (protein kinase A) phosphorylation sites (residues 27–33 and 38–43; Figure 1B).

*Fr*ZIP2 protein has very short N- and C-termini with predicted location on the luminal/outer side of the targeted membrane that is also a conserved feature of most functionally characterized ZIP proteins (Figure 1A), and a typical signature sequence of the ZIP family (FALSAHSVFEGVALG) is identified within TM IV of *Fr*ZIP2 protein (Figure 1B).

Expression of *Fr*ZIP2 proteins in cultured cells

Functional characterization of *Fr*ZIP2 in cultured cells depends on whether the full-size *Fr*ZIP2 protein can be successfully expressed

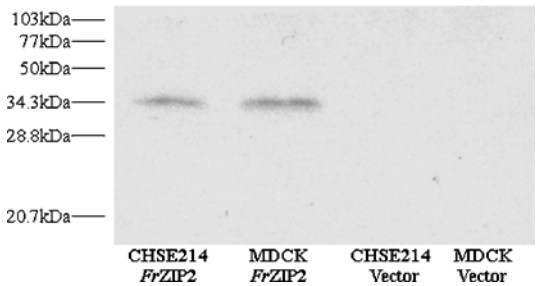

Figure 2 Protein expression of *Fr*ZIP2(H)$_6$ in CHSE214 and MDCK cells

Expression plasmid pIRES2EGFP-*Fr*ZIP2(H)$_6$ was transfected into either CHSE214 or MDCK cells, and the expressed *Fr*ZIP2(H)$_6$ proteins in both cell lines were then detected by SDS-urea/PAGE and Western blotting.

in these cells. To examine the expression of *Fr*ZIP2 protein in cultured cells, we labelled *Fr*ZIP2 ORF with a His$_6$ epitope at its C-terminus, and *Fr*ZIP2(His)$_6$ was subsequently inserted into the mammalian expression plasmid vector, pIRES2EGFP, to generate pIRES2EGFP-*Fr*ZIP2(H)$_6$. After pIRES2EGFP-*Fr*ZIP2(H)$_6$ was transfected into CHSE214 or MDCK cells, SDS-urea/PAGE and Western blotting were performed to immunodetect *Fr*ZIP2(H)$_6$ protein that is expected to be transcriptionally expressed from the human CMV (cytomegalovirus) immediate-early enhancer/promoter and subsequently translated. As shown in Figure 2, a single protein band was detected in lanes containing protein samples from pIRES2EGFP-*Fr*ZIP2(H)$_6$-transfected MDCK and CHSE214 cells, whereas there were no visible protein bands in other lanes containing protein samples from MDCK or CHSE214 cells with the empty plasmid vector, pIRES2EGFP (Figure 2). When being compared with protein markers, the molecular mass of the detected *Fr*ZIP2(H)$_6$ protein is close to 34.3 kDa (Figure 2), which is similar to the predicted *Fr*ZIP2 protein of 34 kDa. The existence of *Fr*ZIP2(H)$_6$ proteins suggests that *Fr*ZIP2(H)$_6$ can be successfully expressed as the full-size protein when transfected into MDCK and CHSE214 cells. Since the only difference between the expression constructs pIRES2EGFP-*Fr*ZIP2(H)$_6$ and pIRES2EGFP-*Fr*ZIP2 is that an epitope of His$_6$ was added at the C-terminus of *Fr*ZIP2 ORF, it can be deduced that *Fr*ZIP2 can be successfully expressed as the full-size protein in both MDCK and CHSE214 cells.

Functional characterization of *Fr*ZIP2 in MDCK cells

To understand the roles of *Fr*ZIP2 in cellular zinc uptake, *Fr*ZIP2 was heterologously expressed and functionally characterized in MDCK cells. This particular cell line was chosen because of its epithelial properties that may be appropriate for functional studies of ZIP zinc uptake transporters (*Fr*ZIP2) in epithelial cells. For the functional expression of *Fr*ZIP2, the *Fr*ZIP2 ORF was cloned into pIRES2EGFP to generate pIRES2EGFP-*Fr*ZIP2 for expression from the CMV promoter. A single bicistronic mRNA containing both *Fr*ZIP2 ORF and EGFP with an internal ribosome entry site in the middle were produced when transfected into cultured cells, and *Fr*ZIP2 and EGFP ORFs were subsequently translated as separate polypeptides. Hence, EGFP could be used as a marker of the stable expression of *FrZIP2* in MDCK cells. Stable MDCK transfectants were generated with the expression of either *Fr*ZIP2 or empty vector, hereafter referred to as MDCK-*Fr*ZIP2 and MDCK-Vec respectively. The stable transfected cells were monitored for green fluorescence using an inverted phase-contrast fluorescence microscope (Nikon Eclipse 200) to ensure the stable expression of *Fr*ZIP2 before $^{65}Zn^{2+}$ flux assays.

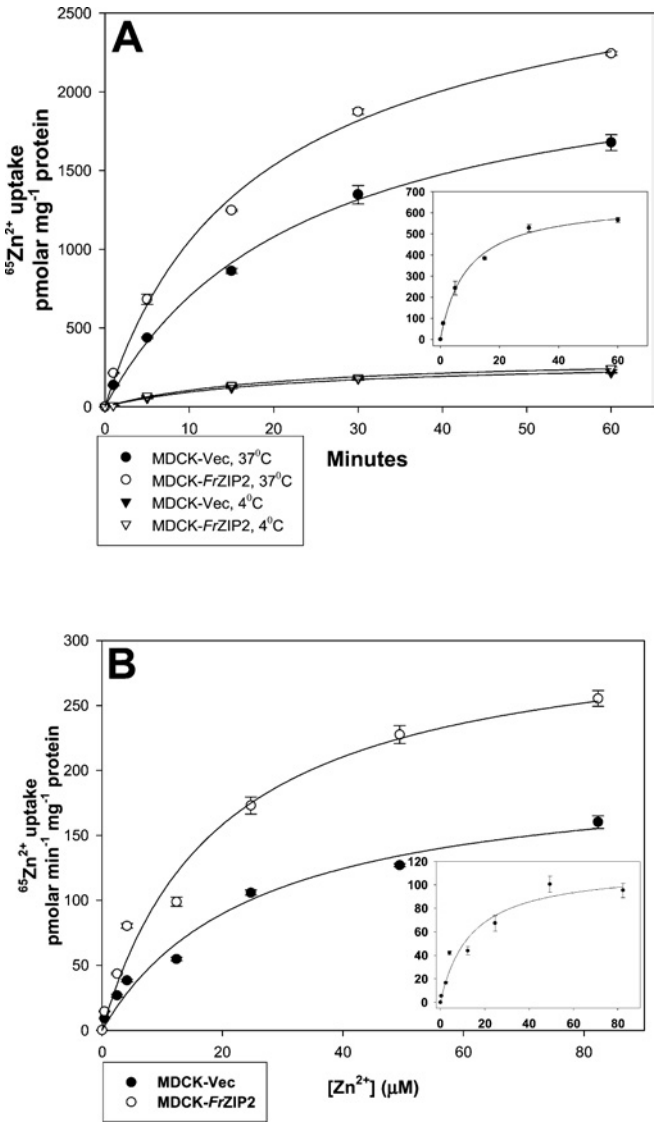

Figure 3 Functional expression of *Fr*ZIP2 in MDCK cells

(**A**) Time and temperature dependences of zinc accumulation assayed in MDCK-*Fr*ZIP2 (open symbols) and MDCK-Vec (filled symbols) cells. The cells were incubated in uptake buffer containing 3 μM $ZnCl_2$ plus 0.028 μCi $^{65}Zn^{2+}$ at 4 °C (triangles) or 37 °C (circles) for 1, 5, 15, 30 or 60 min. The inset shows the time-dependent zinc uptake via *Fr*ZIP2. Values are means ± S.E.M. ($n = 3$). (**B**) Concentration-dependent zinc uptake of MDCK-*Fr*ZIP2 and MDCK-Vec cells. Zinc uptake rate was determined by incubating cells in uptake buffer containing a range of $ZnCl_2$ concentrations at 37 °C for 20 min. The concentration-dependent zinc uptake via *Fr*ZIP2 is shown in the inset. Values are means ± S.E.M. ($n = 3$).

Zinc accumulation in MDCK-Vec cells suggests the existence of an endogenous zinc uptake activity that displays temperature- and time-dependent properties. When MDCK-Vec cells were incubated with uptake buffer containing 3 μM $ZnCl_2$ plus 0.028 μCi $^{65}Zn^{2+}$, only very low levels of $^{65}Zn^{2+}$ accumulation were detected at 4 °C, whereas at 37 °C, $^{65}Zn^{2+}$ accumulation was significantly increased in a typical time-dependent manner (Figure 3A). Similarly, $^{65}Zn^{2+}$ accumulation in MDCK-*Fr*ZIP2 cells was also temperature- and time-dependent. At 4 °C, there was no difference of $^{65}Zn^{2+}$ accumulation between MDCK-*Fr*ZIP2 and MDCK-Vec cells (Figure 3A). However, at 37 °C, MDCK-*Fr*ZIP2 cells accumulated more $^{65}Zn^{2+}$ over a 60 min period than did the MDCK-Vec cells (Figure 3A). Thus the expression of

*Fr*ZIP2 in MDCK cells increased the cellular zinc accumulation in a temperature- and time-dependent way.

Both the endogenous and *Fr*ZIP2-mediated zinc uptake activities in MDCK cells were concentration-dependent and saturable processes. When assayed over a range of zinc concentrations, the endogenous system in MDCK-Vec cells displayed Michaelis–Menten kinetics with an apparent K_m of 25 μM zinc and a J_{max} of 203 pmol zinc $\cdot$ min^{-1} $\cdot$ (mg of protein)$^{-1}$ (Figure 3B). The specific contribution of *Fr*ZIP2 to zinc uptake was estimated by subtracting the uptake rates in vector-only control cells from the corresponding values in MDCK-*Fr*ZIP2 cells, and the *Fr*ZIP2-dependent zinc uptake activity had an apparent K_m of 13.6 μM zinc and a J_{max} of 115 pmol zinc $\cdot$ min^{-1} $\cdot$ (mg of protein)$^{-1}$ (Figure 3B). Thus, based on its temperature-, time- and concentration-dependent properties of zinc uptake, we suggest that *Fr*ZIP2 functions as a zinc uptake transporter when expressed in MDCK cells.

To examine the specificity of the *Fr*ZIP2-dependent activity for zinc over other possible metal substrates, we tested the effects of various metal ions on zinc uptake by MDCK-*Fr*ZIP2 cells. As a control, the metal ion specificity of the endogenous zinc uptake system was also determined in MDCK-Vec cells. The endogenous zinc uptake activity in MDCK-Vec cells was markedly inhibited by 30 μM non-radioactive Zn^{2+}, Cu^{2+}, Cd^{2+}, 1 mM Ca^{2+} or 10 μM La^{3+}, and to a far less extent, by 30 μM Co^{2+}, Fe^{2+} or Fe^{3+} (Figure 4A). In contrast, *Fr*ZIP2-dependent uptake activity was strongly inhibited by excess non-radioactive Zn^{2+} and, surprisingly, completely blocked by Cu^{2+} (Figures 4A and 4B). Ca^{2+} (1 mM) only slightly inhibited the *Fr*ZIP2-dependent zinc uptake activity (Figures 4A and 4B). Like the endogenous zinc uptake system, *Fr*ZIP2-dependent uptake activity was also significantly inhibited by La^{3+} and Cd^{2+}, and to a lesser extent by other metals such as Co^{2+}, Fe^{2+} and Fe^{3+} (Figures 4A and 4B). Thus the *Fr*ZIP2-dependent activity showed a degree of selectivity for zinc, but it seems possible that *Fr*ZIP2 may transport Cu^{2+} and other cations as well.

To understand the biochemical properties of *Fr*ZIP2, we investigated the effects of pH levels in uptake buffer on zinc uptake mediated by both endogenous and *Fr*ZIP2-mediated zinc uptake systems. The endogenous zinc uptake activity peaked at pH between 5.5 and 7.5, and then decreased slightly at pH 8.0 in comparison with those at pH 7.5 and 7.0 (Figure 5A). In marked contrast, *Fr*ZIP2-mediated zinc uptake was completely inhibited at pH levels above 7.0, and reached a peak at pH 6.0–6.5 (Figure 5A).

As a change in pH influences zinc speciation in the uptake buffer, we calculated the concentration of Zn^{2+} ion at each pH using MINEQL+ software (4.0). As shown in Figures 5(B) and 5(C), the free Zn^{2+} ion concentration in uptake buffer decreased with increase in pH. The endogenous zinc uptake activity in MDCK cells was highest between pH 5.5 and 7.5, and did not follow changes of the free Zn^{2+} concentrations (Figure 5B). In contrast, the *Fr*ZIP2-mediated zinc uptake was entirely blocked in uptake buffer at pH 7.5 and 8.0 although the uptake buffer still contained 1.13 and 0.893 μM Zn^{2+} ions respectively (Figure 5C). Conversely, the *Fr*ZIP2-mediated zinc uptake was higher at pH 6.0 and 6.5 than at pH 7.0, while the free Zn^{2+} concentration in uptake buffer was just slightly elevated from 1.19 μM (pH 7.0) to 1.21 μM (pH 6.5) and 1.22 μM (pH 6.0) (Figure 5C). According to the concentration-dependent properties of *Fr*ZIP2-dependent zinc uptake, this slight change of free Zn^{2+} concentration seemed unlikely to influence significantly the zinc accumulation via *Fr*ZIP2, and thus the elevation of *Fr*ZIP2-mediated zinc uptake at pH 6.0 and 6.5 in comparison with pH 7.0 was likely due to the increased acidity in uptake buffer rather than the slight changes of free Zn^{2+} concentration.

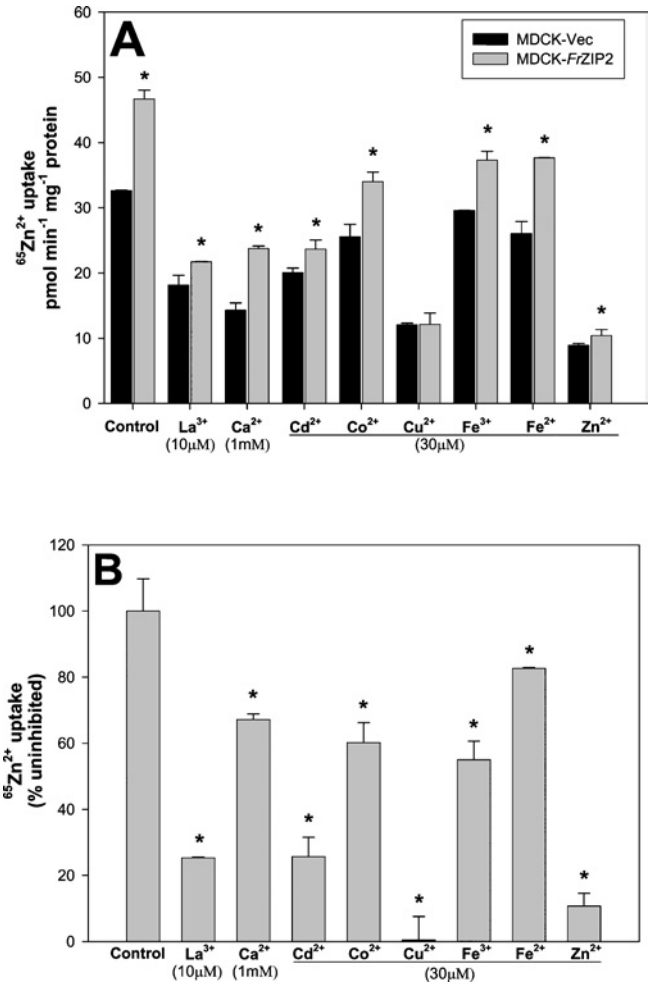

Figure 4 Characterization of metal specificity of *Fr*ZIP2-dependent and endogenous zinc uptake systems in MDCK cells

Excess of the indicated non-radioactive metal ions was added to uptake buffer containing 1.5 μM $ZnCl_2$ plus 0.028 μCi $^{65}Zn^{2+}$, and the cells were incubated under these conditions at 37°C for 20 min before washing and counting. (**A**) Zinc uptake of MDCK-Vec and MDCK-*Fr*ZIP2 cells was measured and compared with cells incubated in the absence of inhibitor (control). Values are means $\pm$ S.E.M. ($n = 3$). (**B**) Inhibition of *Fr*ZIP2-dependent zinc uptake activity by indicated excessive metals. The percentage zinc uptake for each condition was compared with uptake in uncompeted cells (control). Significant differences between experimental groups were tested using non-parametric ANOVA followed by post-hoc test. *$P < 0.05$, significant differences from mock-transfected cells (**A**) or control $^{65}Zn^{2+}$ uptake (**B**).

Both the endogenous and *Fr*ZIP2-mediated zinc uptake activities were inhibited by HCO_3^- (0.5 mM) in uptake buffer (Figure 6). Control experiments showed that this level of HCO_3^- did not change the pH (pH 7.0) in uptake buffer over the duration of the experiment. The addition of 0.5 mM HCO_3^- caused no major change in the free Zn^{2+} ion concentration (1.17 μM) in uptake buffer when compared with that (1.19 μM) in control uptake buffer according to the zinc speciation analysis with MINEQL+ software. This slight change of Zn^{2+} ion concentration by the addition of HCO_3^- seemed unlikely to be the cause of the significant decrease of either endogenous or *Fr*ZIP2-dependent zinc uptake after the addition of HCO_3^- (Figure 6). Thus the inhibition of endogenous and *Fr*ZIP2-mediated zinc uptake activities by the addition of 0.5 mM HCO_3^- probably represented true functional properties of these two zinc uptake systems.

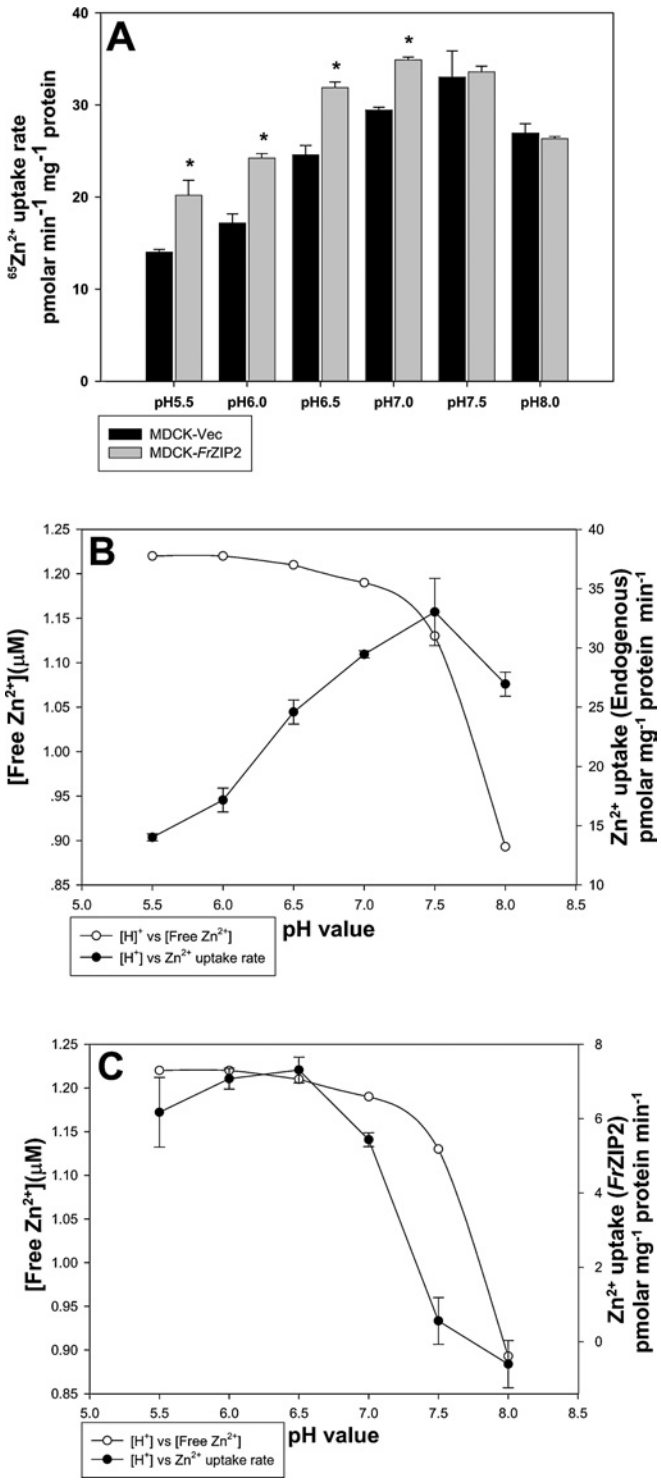

Figure 5 Effects of pH on the endogenous and *Fr*ZIP2-dependent zinc uptake activities in MDCK cells

(**A**) Zinc uptake rate was assayed in MDCK-Vec (black bars) and MDCK-*Fr*ZIP2 cells (grey bars) with 1.5 μM $ZnCl_2$ plus 0.03 μCi $^{65}Zn^{2+}$ in uptake buffer adjusted to the indicated pH. Values are means $\pm$ S.E.M. ($n = 3$). Significant differences between experimental groups were tested using non-parametric ANOVA followed by post-hoc test. *$P < 0.05$, significant differences from control values. (**B**) Effects of pH on free Zn^{2+} concentration and the endogenous zinc uptake activities. (**C**) Effects of pH on free Zn^{2+} concentration and the *Fr*ZIP2-mediated zinc uptake activity that was calculated by subtracting MDCK-Vec rates from the corresponding MDCK-*Fr*ZIP2 values. The free zinc concentration in uptake buffer with different pH values was analysed with MINEQL+ software.

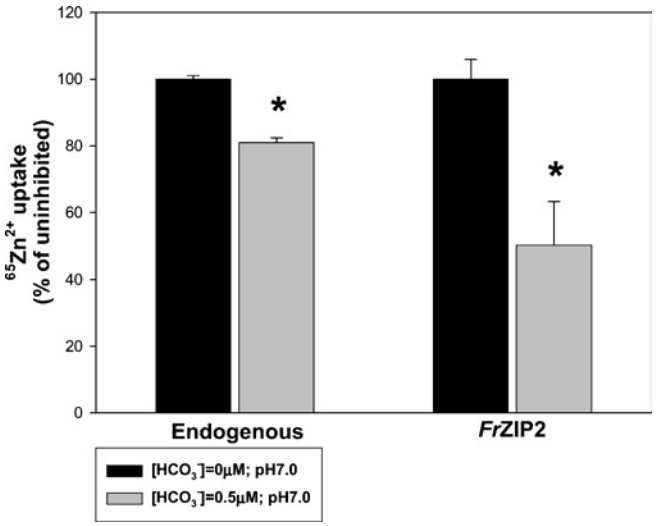

Figure 6 HCO_3^- effects on endogenous and *Fr*ZIP2-mediated zinc uptake activities in MDCK cells

Zinc uptake was assayed in MDCK-Vec (black bars) and MDCK-*Fr*ZIP2 cells (grey bars) with flux buffer containing 1.5 μM $ZnCl_2$ plus 0.03 μCi $^{65}Zn^{2+}$ and either 0 mM (control) or 0.5 mM $NaHCO_3$. Percentage zinc uptake with 0.5 mM $NaHCO_3$ was compared with uptake in cells without added $NaHCO_3$. Values are means $\pm$ S.E.M. ($n = 3$). The statistical significance of differences was determined using Mann–Whitney U-test. *Significant differences from control values ($P < 0.05$).

Tissue distribution of *Fr*ZIP2 mRNA

RT–PCR was performed to examine the expression levels of *Fr*ZIP2 mRNA in the gill, intestine, kidney and ovary of *Fugu* pufferfish. According to our results, the highest level of *Fr*ZIP2 mRNA was detected in the ovary and intestine, and the lowest in the kidney (Figure 7). Pufferfish gill contains an intermediate amount of *Fr*ZIP2 mRNA (Figure 7).

DISCUSSION

Zinc uptake across the apical membrane of absorptive epithelial cells is the first gate to regulate zinc homoeostasis, and thus it is very important to understand the molecular mechanisms of cellular zinc uptake. In mammals, SLC39A4 seems to mediate dietary zinc uptake in the intestine [12–14,18,19]. However, probably there are alternative pathways for zinc uptake in mammalian intestines as dysfunctional ZIP4 only impairs zinc uptake and does not completely abrogate the dietary zinc absorption [18,19]. While the existence of a fish SLC39A4 orthologue remains uncertain, ZIP1 protein seems to be a constitutive high-affinity zinc uptake transporter in various tissues of both zebrafish and *Fugu* pufferfish [22], and ECaC appears to be the candidate protein mediating the reciprocally competitive uptake of calcium and zinc in the gill [23]. In the present study, to understand other zinc uptake pathways that mediate zinc uptake in fish gill and intestine, we molecularly cloned and functionally characterized a second fish member of the ZIP subfamily II, *Fr*ZIP2, from *Fugu* pufferfish gill.

Structural characterization suggested that *Fr*ZIP2 is a fish member of the ZIP subfamily II. Just like most of the functionally characterized ZIP protein in fungi, plants and mammals [11], *Fr*ZIP2 protein exhibits all the conserved features of ZIP subfamilies I and II, including eight TM domains, a potential metal-binding domain between TM III and IV, functionally important

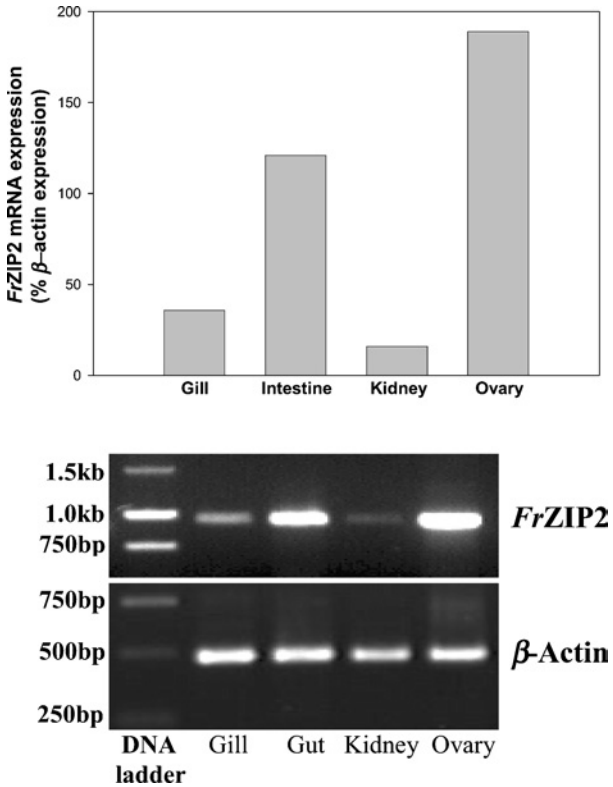

Figure 7 Distribution of *Fr*ZIP2 mRNA in various tissues of pufferfish by RT–PCR

Upper panel: relative levels of *Fr*ZIP2 mRNA in pufferfish gill, intestine, kidney and ovary normalized by β-actin mRNA using SigmaGel software (Jandel Scientific). Lower panel: expression pattern of *Fr*ZIP2 and β-actin mRNA in agarose gels.

histidine residues in the amphipathic TM IV and V etc. Furthermore, *Fr*ZIP2 shares much higher amino acid identity with individual members of the ZIP subfamily II than those in the ZIP subfamilies I, III and IV, suggesting that it belongs to the ZIP subfamily II. In particular, the highest amino acid identity ($\sim$60 %) exists throughout *Fr*ZIP2 and mammalian SLC39A3 proteins, especially in the regions of eight TM domains. Thus, together with the observation that mouse SLC39A3 functions as a zinc uptake transporter when expressed in HEK-293 cells [17], these structural properties support our initial hypothesis that *Fr*ZIP2 is another zinc uptake transporter in pufferfish along with *Fr*ZIP1.

Functional characterization in MDCK cells renders further supportive evidence that *Fr*ZIP2 can mediate uptake of zinc. *Fr*ZIP2 facilitated cellular zinc uptake in a temperature-, time-, concentration- and pH-dependent manner in MDCK cells. In comparison, the apparent K_m of *Fr*ZIP2 for zinc uptake (13.6 μM Zn^{2+}) is significantly lower than the endogenous uptake system of MDCK cells (25 μM Zn^{2+}) was similar to that of the yeast low-affinity zinc uptake transporter ZRT2 [31], and markedly higher than those of the yeast and zebrafish high-affinity zinc uptake transporters ZRT1 (1 μM Zn^{2+}) [32] and *Dr*ZIP1 (<0.5 μM Zn^{2+}) [22], human SLC39A1 and SLC39A2 (3 μM Zn^{2+}) and mouse SLC39A1–SLC39A3 (1.5 μM Zn^{2+}) [15–17]. Furthermore, we recently showed that *Fr*ZIP2 protein displayed much lower zinc binding affinity than the orthologue of *Fr*ZIP1 in zebrafish, *Dr*ZIP1 (eight times lower) [22]. Thus *Fr*ZIP2 appears to be a low-affinity zinc uptake transporter in *Fugu* pufferfish.

As would be expected from a zinc influx protein, *Fr*ZIP2-mediated uptake of ^{65}Zn in transfected MDCK cells was greatly inhibited by 20-fold excess of non-radioactive zinc. Surprisingly however, *Fr*ZIP2-mediated ^{65}Zn uptake was completely quenched by 20-fold excess of Cu^{2+}. This suggests that *Fr*ZIP2 might transport Cu^{2+} as well as Zn^{2+}. A similar phenomenon was also observed in *Arabidopsis* ZIP2 (*At*ZIP2) and human SLC39A2. A 10-fold excess of Cu^{2+} inhibited zinc uptake of *At*ZIP2 to the same extent as a 10-fold of non-radioactive Zn^{2+} [33], and zinc uptake by human SLC39A2 was also greatly inhibited by Cu^{2+} [15]. Interestingly, a distinct pathway of copper transport (Cu^{2+}) was identified in Ctr1-homozygous knockout mouse embryonic cells, which exhibited approx. 30 % residual copper transport activity that was a saturable process with a K_m of approx. 10 μM Cu^{2+} and with biochemical features distinct from that of Ctr1 [34]. Furthermore, 50-fold excess of zinc markedly inhibited this Cu^{2+} uptake pathway, while it exhibited no effects on the Cu^{+} uptake mediated by Ctr1 [34], suggesting that this copper uptake pathway may be related to cellular zinc uptake. Consistently, physiological evidence indicates that the intestinal zinc uptake pathway in mammals and fish may also be used for Cu^{2+} transport as Cu^{2+} status has a considerable effect on zinc absorption and vice versa [35–37], which is further supported by the observation that the endogenous zinc uptake in MDCK cells was also inhibited by Cu^{2+}. Human SLC39A1, SLC39A2 and the divalent metal transporter (DMT1, SLC40A1) were considered unlikely to have a role in mediating Cu^{2+} uptake [34], but SLC39A3 remains a candidate. Thus it would be interesting to investigate if *Fr*ZIP2 and its close homologues in mammals, SLC39A3, can mediate cellular Cu^{2+} uptake.

Both MDCK endogenous and *Fr*ZIP2-mediated zinc uptake activities were inhibited by La^{3+} and Cd^{2+}. La^{3+} is known to be a calcium channel blocker. It blocks ECaC-mediated calcium transport and inhibits both calcium and zinc uptake in rainbow-trout gill [4,38]. From the present results, it appears that La^{3+} blocks the *Fr*ZIP2-mediated zinc uptake activity as well. The inhibitory effect of Cd^{2+} on *Fr*ZIP2-mediated zinc uptake is consistent with the fact that waterborne Cd^{2+} reduces branchial zinc influx in fish and competitively inhibits zinc uptake in cultured mammalian cells [39].

Ca^{2+} (1 mM) had little effect on *Fr*ZIP2-mediated zinc uptake while it inhibited the endogenous zinc uptake activity in MDCK cells by approx. 50 %. A common pathway for zinc and calcium uptake has been identified in fish gills [38] and in rat, piglet and pig enterocytes [40–42]. ECaC appears to be the candidate protein mediating the common pathway for zinc and calcium uptake in fish gill [23], but it still remains unknown if the mammalian ECaC orthologues fulfil the same functions in mammalian cells as well.

Like human SLC39A1 [16], zinc uptake via *Fr*ZIP2 was inhibited by 0.5 mM HCO_3^-. This property is different from that of human SLC39A2 that zinc uptake activity of human SLC39A2 was stimulated by 0.5 mM HCO_3^- [15], suggesting that *Fr*ZIP2 may employ a different mechanism of zinc translocation from human SLC39A2. A Zn^{2+}/HCO_3^- symport mechanism has been proposed on the zinc transport activity of human SLC39A2 [15]. This does not appear to be the mechanism by which zinc is translocated across the cell membrane by *Fr*ZIP2. Instead, experimental data from the present study indicate that a proton-driven mechanism of zinc transport may be a possibility.

*Fr*ZIP2 also exhibited a different pH dependence from human SLC39A2. Zinc uptake by human SLC39A2 was inhibited at pH levels below 7.0 and stimulated at higher pH [15]. In marked contrast, *Fr*ZIP2-mediated zinc uptake was markedly reduced at pH levels above 7.0, and reached a peak at about pH 6.0 and 6.5. This different pH dependence further suggests that *Fr*ZIP2 employs a different mechanism of zinc transport from that of human SLC39A2, and that the H^+ gradient across the cell membrane

might provide partial driving force for zinc translocation via *Fr*ZIP2. In accordance with the pH dependence of *Fr*ZIP2, a slightly reduced water pH has been observed to increase the movement of zinc across the gill into the body in fish [43]. Coupled with the expression of *Fr*ZIP2 mRNA in pufferfish gill, this concurrence of pH dependence of *Fr*ZIP2 and physiology of branchial zinc uptake in fish suggests that *Fr*ZIP2 may be a molecular mechanism of branchial zinc acquisition in *Fugu* pufferfish.

Substantial expression of *Fr*ZIP2 mRNA was detected in the intestine, suggesting that *Fr*ZIP2 may be an important pathway of cellular zinc uptake in the *Fugu* pufferfish intestine as well. Consistent with the consensus that fish intestine is the bulk pathway of zinc absorption under standard dietary conditions and gills may act to supplement absorption when required [4], pufferfish intestine contains a higher level of *Fr*ZIP2 mRNA than the gill. In contrast, *Fr*ZIP2 mRNA was detected at a very low level in pufferfish kidney. In marine teleosts, the kidneys mainly function to excrete bivalent ions such as calcium, magnesium and phosphate [44]. Although the renal zinc metabolism in fish is still unknown, the low level of renal *Fr*ZIP2 mRNA is consistent with the major roles of kidney in ion homoeostasis in marine fish. The highest level of *Fr*ZIP2 mRNA was found in the ovary among the four pufferfish tissues herein studied. This is consistent with previous findings that considerable quantities of zinc are needed for the developing oocytes [45,46]. In accordance with this, mouse slc39A1 and slc39A2 are expressed at relatively high levels in the ovary [17]. Interestingly, mouse slc39A3 seems to be expressed preferentially in testes [17]. Slc39A3 is also expressed in mammary glands of the rat during mid lactation [47]. Furthermore, as the zinc concentration of the milk decreased during the course of lactation, levels of slc39A3 mRNA and SLC39A3 protein decreased concomitantly, indicating that rat SLC39A3 may be involved in the transport of zinc into milk. Clearly, zinc transporters are important throughout development and different members of the slc30A and slc39A families are expressed in a time- and tissue-specific manner. Such a subfunctionalization may have provided the evolutionary advantage that allowed the many members of these families to co-exist.

This work was supported by K. C. Wong Education Foundation (The landmark square, Hong Kong, People's Republic of China), A. Q. was supported by a Chinese Scholarship council (Beijing, People's Republic of China) and an U.S. EPA grant R 826104-01-1 (to C. H.).

REFERENCES

1 Vallee, B. L. and Auld, D. S. (1990) Zinc coordination, function, and structure of zinc enzymes and other proteins. Biochemistry **29**, 5647–5659

2 MacDiarmid, C. W., Gaither, L. A. and Eide, D. J. (2000) Zinc transporters that regulate vacuolar zinc storage in *Saccharomyces cerevisiae*. EMBO J. **19**, 2845–2855

3 Frederickson, C. J. and Bush, A. I. (2001) Synaptically released zinc: physiological functions and pathological effects. Biometals **14**, 353–366

4 Hogstrand, C. and Wood, C. M. (1996) The physiology and toxicology of zinc in fish. In Toxicology of Aquatic Pollution. In (Taylor, E. W., ed.), pp. 61–84, Cambridge University Press, Cambridge

5 Bury, N. R., Walker, P. A. and Glover, C. N. (2003) Nutritive metal uptake in teleost fish. J. Exp. Biol. **206**, 11–23

6 Gaither, L. A. and Eide, D. J. (2001) Eukaryotic zinc transporters and their regulation. Biometals **14**, 251–270

7 Taylor, K. M. and Nicholson, R. I. (2003) The LZT proteins; the LIV-1 subfamily of zinc transporters. BBA Biomembranes **1611**, 16–30

8 Lioumi, M., Ferguson, C. A., Sharpe, P. T., Freeman, T., Marenholz, I., Mischke, D., Heizmann, C. and Ragoussis, J. (1999) Isolation and characterization of human and mouse ZIRTL, a member of the IRT1 family of transporters, mapping within the epidermal differentiation complex. Genomics **62**, 272–280

9 MacDiarmid, C. W., Gaither, L. A. and Eide, D. J. (2000) Zinc transporters that regulate vacuolar zinc storage in *Saccharomyces cerevisiae*. EMBO J. **19**, 2845–2855

10 Taylor, K. M., Morgan, H. E., Johnson, A. and Nicholson, R. I. (2003) Structure-function analysis of HKE4, a member of the new LIV-1 subfamily of zinc transporters. Biochem. J. **377**, 131–139

11 Eide, D. J. (2004) The SLC39 family of metal ion transporters. Pflugers Arch. Eur. J. Physiol. **447**, 796–800

12 Dufner-Beattie, J., Wang, F. D., Kuo, Y. M., Gitschier, J., Eide, D. and Andrews, G. K. (2003) The *Acrodermatitis enteropathica* gene ZIP4 encodes a tissue-specific, zinc regulated zinc transporter in mice. J. Biol. Chem. **278**, 33474–33481

13 Wang, K., Zhou, B., Kuo, Y. M., Zemansky, J. and Gitschier, J. (2002) A novel member of a zinc transporter family is defective in *Acrodermatitis enteropathica*. Am. J. Hum. Genet. **71**, 66–73

14 Küry, S., Dréno, B., Bézieau, S., Giraudet, S., Kharfi, M., Kamoun, R. and Moisan, J. P. (2002) Identification of *SLC39A4*, a gene involved in *Acrodermatitis enteropathica*. Nat. Genet. **31**, 239–240

15 Gaither, L. A. and Eide, D. J. (2000) Functional expression of the human hZIP2 zinc transporter. J. Biol. Chem. **275**, 5560–5564

16 Gaither, L. A. and Eide, D. J. (2001) The human ZIP1 transporter mediates zinc uptake in human K562 erythroleukemia cells. J. Biol. Chem. **276**, 22258–22264

17 Dufner-Beattie, J., Langmade, S. J., Wang, F., Eide, D. J. and Andrews, G. K. (2003) Structure, function, and regulation of a subfamily of mouse zinc transporter genes. J. Biol. Chem. **278**, 50142–50150

18 Liuzzi, J. P., Bobo, J. A., Lichten, L. A., Samuelson, D. A. and Cousins, R. J. (2004) Responsive transporter genes within the murine intestinal–pancreatic axis form a basis of zinc homeostasis. Proc. Natl. Acad. Sci. U.S.A. **101**, 14355–14360

19 Cragg, R. A., Philips, S. R., Piper, J. M., Varma, J. S., Campbell, J. C., Mathers, J. C. and Ford, D. (2005) Homeostatic regulation of zinc transporters in the human small intestine by dietary zinc supplementation. Gut **54**, 469–478

20 Wang, F. D., Dufner-Beattie, J., Kim, B. E., Petris, M. J., Andrews, G. and Eide, D. J. (2004) Zinc stimulated endocytosis controls activity of the mouse ZIP1 and ZIP3 zinc uptake transporters. J. Biol. Chem. **279**, 24631–24639

21 Kim, B. E., Wang, F., Dufner-Beattie, J., Andrews, G. K., Eide, D. J. and Petris, M. J. (2004) Zn^{2+}-stimulated endocytosis of the mZIP4 zinc transporter regulates its location at the plasma membrane. J. Biol. Chem. **279**, 4523–4530

22 Qiu, A., Shayeghi, M. and Hogstrand, C. (2005) Molecular cloning and functional characterisation of a high affinity zinc importer (*Dr*ZIP1) from zebrafish, *Danio rerio*. Biochem. J. **388**, 745–754

23 Qiu, A. and Hogstrand, C. (2004) Functional characterisation and genomic analysis of an epithelial calcium channel (ECaC) from pufferfish, *Fugu rubripes*. Gene **342**, 113–123

24 Aparicio, S., Chapman, J., Stupka, E., Putnam, N., Chia, J.-M., Dehal, P., Christoffels, A., Rash, S., Hoon, S., Smit, A. et al. (2002) Whole-genome shotgun assembly and analysis of the genome of *Fugu rubripes*. Science **297**, 1301–1310

25 Dolphin, C. T., Cullingford, T. E., Shephard, E. A., Smith, R. L. and Phillips, I. R. (1996) Differential developmental and tissue-specific regulation of expression of the genes encoding three members of the flavin-containing monooxygenase family of man, FMO1, FM03 and FM04. Eur. J. Biochem. **235**, 683–689

26 Higgins, D., Thompson, J., Gibson, T., Thompson, J. D., Higgins, D. G. and Gibson, T. J. (1994) CLUSTAL W: improving the sensitivity of progressive multiple sequence alignment through sequence weighting, position-specific gap penalties and weight matrix choice. Nucleic Acids Res. **22**, 4673–4680

27 Moller, S., Croning, M. D. R. and Apweiler, R. (2001) Evaluation of methods for the prediction of membrane spanning regions. Bioinformatics **17**, 646–653

28 Kreegipuu, A., Blom, N. and Brunak, S. (1999) PhosphoBase, a database of phosphorylation sites: release 2.0. Nucleic Acids Res. **27**, 237–239

29 Guerinot, M. L. (2000) The ZIP family of metal transporters. BBA Biomembranes **1465**, 190–198

30 Berg, J. M. and Shi, Y. G. (1996) The galvanisation of biology: a growing application for the roles of zinc. Science **271**, 1081–1085

31 Zhao, H. and Eide, D. (1996) The ZRT2 gene encodes the low affinity zinc transporter in *Saccharomyces cerevisiae*. J. Biol. Chem. **271**, 23203–23210

32 Zhao, H. and Eide, D. (1996) The yeast ZRT1 gene encodes the zinc transporter protein of a high-affinity uptake system induced by zinc limitation. Proc. Natl. Acad. Sci. U.S.A. **93**, 2454–2458

33 Grotz, N., Fox, T., Connolly, E., Park, W., Guerinot, M. L. and Eide, D. J. (1998) Identification of a family of zinc transporter genes from *Arabidopsis* that respond to zinc deficiency. Proc. Natl. Acad. Sci. U.S.A. **95**, 7220–7224

34 Lee, J., Petris, M. J. and Thiele, D. J. (2002) Characterization of mouse embryonic cells deficient in the ctr1 high affinity copper transporter: identification of a ctr1-independent copper transport system. J. Biol. Chem. **277**, 40253–40259

35 Mills, C. F. (1986) The influence of chemical species on the adsorption and physiological utilization of trace elements from the diet or environment. In The Importance of Chemical 'Speciation' in Environmental Processes (Bernhard, M., Brinckman, F. E. and Sadler, P. J., eds.), pp. 71–83, Springer-Verlag, Berlin/Heidelberg
36 Linder, M. C. (1991) Biochemistry of Copper, pp. 15–161, Plenum Press, New York
37 Glover, C. N. and Hogstrand, C. (2003) Effects of dissolved metals and other hydrominerals on *in vivo* intestinal zinc uptake in freshwater rainbow trout. Aquat. Toxicol. **62**, 281–293
38 Hogstrand, C., Verbost, P. M., Bonga, S. E. W. and Wood, C. M. (1996) Mechanisms of zinc uptake in gills of freshwater rainbow trout: interplay with calcium transport. Am. J. Physiol. Reg. **270**, R1141–R1147
39 Reyes, J. G. (1996) Zinc transport in mammalian cells. Am. J. Physiol. Cell Physiol. **39**, C401–C410
40 Rothbassell, H. A. and Clydesdale, F. M. (1991) The influence of zinc, magnesium, and iron on calcium uptake in brush-border membrane-vesicles. J. Am. Coll. Nutr. **10**, 44–49
41 Gunshin, H., Noguchi, T. and Naito, H. (1991) Effect of calcium on the zinc uptake by brush-border membrane-vesicles isolated from the rat small intestine. Agr. Biol. Chem. Tokyo **55**, 2813–2816
42 Bertolo, R. F., Brttger, W. J. and Atkinson, S. A. (2001) Calcium competes with zinc for a channel mechanism on the brush border membrane of piglet intestine. J. Nutr. Biochem. **12**, 66–72
43 Bradley, R. W. and Sprague, J. B. (1985) Accumulation of zinc by rainbow-trout as influenced by pH, water hardness and fish size. Environ. Toxicol. Chem. **4**, 685–694
44 Nishimura, H. and Imai, M. (1982) Control of renal-function in fresh-water and marine teleosts. Fed. Proc. **41**, 2355–2360
45 Fletcher, G. L. and King, M. J. (1978) Seasonal dynamics of Cu^{2+}, Zn^{2+}, Ca^{2+}, and Mg^{2+} in gonads and liver of winter flounder (*Pseudopleuronectes americanus*) – evidence for summer storage of Zn^{2+} for winter gonad development in females. Can. J. Zool. **56**, 284–290
46 Thompson, E. D., Mayer, G. D., Balesaria, S., Glover, C. N., Walsh, P. J. and Hogstrand, C. (2003) Physiology and endocrinology of zinc accumulation during the female squirrelfish reproductive cycle. Comp. Biochem. Physiol. A Mol. Integ. Physiol. **134**, 819–828
47 Kelleher, S. L. and Lonnerdal, B. (2003) Zn transporter levels and localization change throughout lactation in rat mammary gland and are regulated by Zn in mammary cells. J. Nutr. **133**, 3378–3385

Received 6 April 2005/19 May 2005; accepted 20 May 2005
Published as BJ Immediate Publication 20 May 2005, doi:10.1042/BJ20050568